Wireless Neural/EMG Telemetry Systems for Small Freely Moving Animals

Reid R. Harrison, *Member, IEEE*, Haleh Fotowat, *Member, IEEE*, Raymond Chan, Ryan J. Kier, *Member, IEEE*, Robert Olberg, Anthony Leonardo, and Fabrizio Gabbiani

***Abstract*—We have developed miniature telemetry systems that capture neural, EMG, and acceleration signals from a freely moving insect or other small animal and transmit the data wirelessly to a remote digital receiver. The systems are based on custom low-power integrated circuits (ICs) that amplify, filter, and digitize four biopotential signals using low-noise circuits. One of the chips also digitizes three acceleration signals from an off-chip microelectromechanical-system accelerometer. All information is transmitted over a wireless ~900-MHz telemetry link. The first unit, using a custom chip fabricated in a 0.6-μm BiCMOS process, weighs 0.79 g and runs for two hours on two small batteries. We have used this system to monitor neural and EMG signals in jumping and flying locusts as well as transdermal potentials in weakly swimming electric fish. The second unit, using a custom chip fabricated in a 0.35-μm complementary metal–oxide semiconductor CMOS process, weighs 0.17 g and runs for five hours on a single 1.5-V battery. This system has been used to monitor neural potentials in untethered perching dragonflies.**

***Index Terms*—EMG amplifier, neural amplifier, neuroscience, wireless telemetry.**

I. Introduction

MODERN neuroscience research often relies on experiments using small animals, such as mice, fish, and insects. For example, flying insects possess highly capable visual systems that perform complex, real-time calculations to modulate flight control [1], [2]. The study of insect visual processing during the past half century has provided rich insight into biological information-processing strategies.

Measuring the weak extracellular electrical activity produced by neurons (typically in the range of 100 μV–1 mV) or electromyograms (EMGs) in muscles (typically in the range of 1–10 mV) by traditional means has required large rack-mounted amplifiers and data-acquisition systems. Due to the long wires connecting electrodes to remote amplifiers, most electrophysiology experiments must be performed inside a Faraday cage to achieve acceptable signal quality. Animals must be head-fixed or tethered during these experiments, which restricts the simultaneous study of neural activity and behavior.

As electronics have been miniaturized, efforts have been made to create small, lightweight amplifiers and wireless transmitters to permit electrophysiological monitoring during free behavior. Early designs used discrete components to provide analog frequency-modulation (FM) telemetry of EMG signals from flying locusts and moths [3]–[6]. Some systems used discrete components as well as standard off-the-shelf integrated circuits (ICs) (e.g., operational amplifier chips) to transmit neural signals from birds and walking insects [7], [8]. In 2005, Mohseni and colleagues described a three-channel neural telemetry system built around a custom IC and employing the familiar analog FM transmission scheme with time-division multiplexing to separate the channels [9]. Simple RF beacons have been created to track dragonfly migration [10]. More recently, ICs also have been used to stimulate neurons in flying moths [11], [12].

To facilitate more sophisticated investigations into the neural control of behavior, we have developed ICs capable of amplifying two neural signals and two EMG signals from extracellular electrodes, digitizing these signals, adding parity bits for error detection, and wirelessly transmitting the digital information while operating from small, low-mass batteries. We have developed two telemetry systems—version 1 and version 2—using ICs fabricated in 0.6-μm and 0.35-μm technologies, respectively. The first version requires a higher supply voltage (and, thus, increased mass due to batteries) than the second version, but can support an off-chip accelerometer.

II. Version 1 Telemetry System Design

A. IC Design

We designed a custom IC for the version 1 telemetry system, first reported in [13] in a commercially available 0.6-μm BiCMOS process. Using low-mass batteries imposes severe power limits on the design of the chip: small batteries have low capacities and high internal resistance; pulling too much

Manuscript received October 14, 2010; revised February 01, 2011; accepted March 06, 2011. Date of current version May 18, 2011. This work was supported in part by AFRL under contract #FA8651-07-1-0007, in part by the National Science Foundation under Contract NSF-IOB-0516775, in part by the Human Frontier Science Program under contract HFSP-RGP0016, in part by the Grass Foundation, and in part by the Howard Hughes Medical Institute. Vertebrate experimental procedures were performed in accordance with the Marine Biological Laboratory IACUC-approved protocol. This paper was recommended by Associate Editor S. Chakrabartty.

R. R. Harrison was with the Department of Electrical and Computer Engineering and the Department of Bioengineering, University of Utah, Salt Lake City, UT 84112 USA. He is now with Intan Technologies, Los Angeles, CA 90045 USA.

H. Fotowat was with the Baylor College of Medicine, Houston, TX 77030 USA. She is now with the Department of Biology, McGill University, Montreal, QC H3A 1B1, Canada.

R. Chan and F. Gabbiani are with the Department of Neuroscience, Baylor College of Medicine, Houston, TX 77030 USA.

R. J. Kier was with the University of Utah, Salt Lake City, UT 84112 USA. He is now with SiFlare, Sandy, UT 84070 USA.

R. Olberg is with the Department of Biology, Union College, Schenectady, NY 12308 USA.

A. Leonardo is with the Janelia Farm Research Campus, Howard Hughes Medical Institute, Ashburn, VA 20147 USA.

Color versions of one or more of the figures in this paper are available online at http://ieeexplore.ieee.org.

Digital Object Identifier 10.1109/TBCAS.2011.2131140

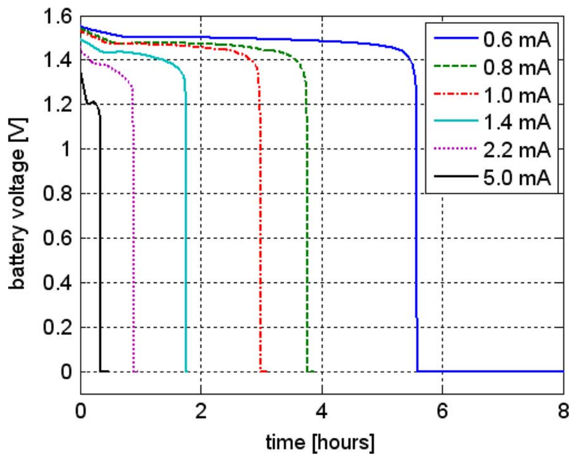

Fig. 1. Measured battery life of an Energizer 337 1.5-V silver–oxide battery (mass = 130 mg) powering a load that draws constant dc current.

current can cause a battery's voltage to collapse immediately, regardless of its stated capacity. After testing many battery types, we opted to use 1.5-V silver–oxide batteries (Energizer 337) having a mass of 130 mg each and a volume of 29 mm^3. While these batteries have a stated capacity of 8.3 mAh, experiments using a constant-current load revealed that drawing 1 mA from the battery reduces its capacity to 3 mAh (see Fig. 1). Currents greater than 2 mA cause large drops in battery voltage and cannot be used. We use two batteries to provide a 3.0-V supply to the version 1 telemetry chip.

Four fully integrated low-noise amplifiers (LNAs) (see Fig. 2) are used to boost and filter the neural and EMG signals obtained from differential electrodes. Three operational transconductance amplifiers (OTAs) used in the circuit are current-mirror OTAs designed for low-noise operation by proper sizing of differential pair and current mirror transistors [14]. The gain of the first stage is set by the $\mathrm{C_1/C_2}$ ratio; the second-stage gain is set by $\mathrm{C_3/C_4}$. Bias generators set the high-frequency cutoff (through $\mathrm{G_{m1}}$ and $\mathrm{G_{m2}}$) and low-frequency cutoff (through $\mathrm{G_{m3}}$) of each amplifier. The $\mathrm{G_{m3}}$ OTA was placed in the second stage so its noise contribution is attenuated by $\mathrm{C_1/C_2}$ when referred to the input [15]. The gain of the EMG amplifiers was set to 100; the gain of the neural amplifiers was set to 1000. The measured CMRR at 1 kHz (averaged across 10 amplifiers) was 74 dB; the PSRR was 63 dB.

A 9-b successive-approximation register (SAR) ADC with capacitive DAC is used to digitize the amplified waveforms. A state machine controls an analog multiplexer and samples the neural signals at a faster rate (11.52 kSamples/s) than the slower EMG signals (1.92 kSamples/s). The ADC also samples (at 1.92 kSamples/s) three auxiliary input pins that are used to interface a commercially available 3-axis MEMS accelerometer (Analog Devices ADXL330) with the chip to provide information on insect movement. The sampling rates are set by a low-power crystal oscillator using an off-chip 11.0592-MHz quartz crystal and drawing only 65 μA from the supply. For every 9-b sample, a parity bit is added to permit error detection. Frame marker bits are added, and the resulting 345.6-kb/s serial bitstream is passed to an on-chip frequency-shift keying (FSK) transmitter

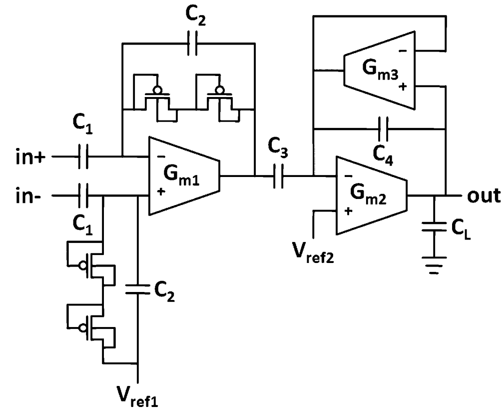

Fig. 2. Schematic of the low-noise biopotential amplifier. Operational transconductance amplifiers (OTAs) are designed according to [14].

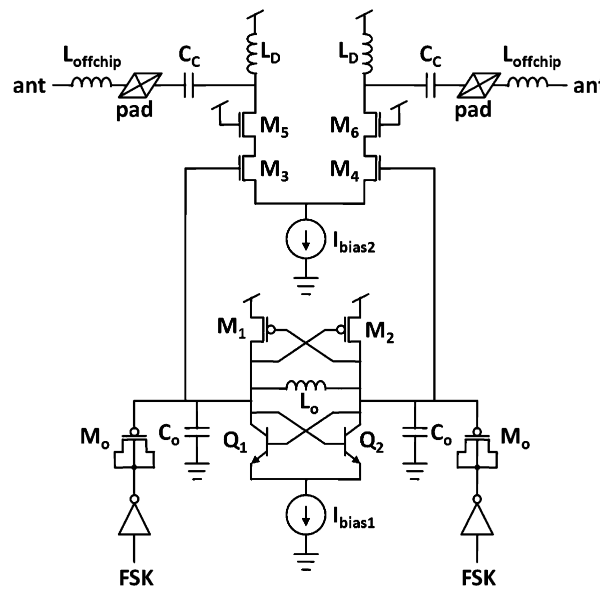

Fig. 3. Schematic of the 920-MHz FSK transmitter. Varactors $(\mathrm{M_o})$ shift the resonant frequency of an open-loop negative-resistance *LC* oscillator.

TABLE I
TELEMETRY CHANNEL SPECIFICATIONS

Data Channel	Band-width	ADC Sampling Rate	Max. Range	ADC V_{LSB}	Input-Referred Noise
Neural Amps 1,2	300Hz-5.2kHz	11.52 kS/s	±1.2mV	4.69µV	2.3 μV_{rms}
EMG Amps 1,2	20Hz-280Hz	1.92 kS/s	±12mV	46.9µV	25 μV_{rms}
Acceler. X,Y,Z	DC-500 Hz	1.92 kS/s	±3.0g[1]	15.6mg	7.8 mg_{rms} (X,Y) 9.8 mg_{rms} (Z)

[1] 1 g = 9.81 m/s^2

(see Fig. 3). Table I summarizes the dynamic range, bandwidth, sampling rate, and input-referred noise of each channel.

The core of the 920-MHz transmitter is an *LC* oscillator that uses a thick top metal layer to build a low-loss 26-nH inductor $\mathrm{L_o}(Q \approx 11)$. The use of a tank with a high *LQ* product, along with vertical *npn* transistors ($\mathrm{Q_1}$ and $\mathrm{Q_2}$) providing a high g_m/I ratio with relatively low parasitic capacitance allows this circuit

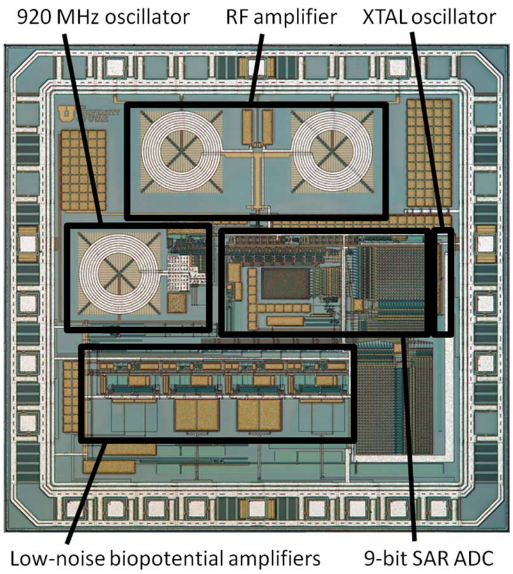

Fig. 4. Die photograph of 2.57×2.48 mm^2 version 1 insect telemetry chip, fabricated in a 0.6-μm BiCMOS process.

to oscillate reliably with a bias current of only 180 μA. Small metal–oxide semiconductor (MOS) varactors $(\mathrm{M_o})$ are used to create a 600-kHz frequency deviation in response to a binary input. To save power, a phase-locked loop (PLL) was not implemented and the oscillator operates in open loop. The measured frequency drift with supply voltage was -2.8 ppm/mV. The batteries have a very flat discharge curve, so frequency drift over time is measureable but not severe. A differential RF output stage with on-chip drain inductors ($\mathrm{L_d} = 26$ nH) and series capacitors ($\mathrm{C_C} = 10$ pF) is connected to an off-chip dipole antenna. Off-chip 56-nH inductors are used to improve radiation from the electrically short dipole. A die photograph of the 2.57×2.48 mm^2 chip is shown in Fig. 4.

B. System-Level Design

Chips were packaged in a molded plastic 28-lead 5×5 mm^2 QFN package and mounted on a 13×9 mm^2 printed-circuit board (PCB) along with battery holders, an accelerometer, crystal, and antenna (see Fig. 5). The complete system with batteries weighs 0.79 g. The chip consumes 880 μA of current and the accelerometer consumes 320 μA, for a total of 1.2 mA. This limits battery life to 2 h of continuous use. The telemetry system can be temporarily mounted to an insect using wax, and electrode wires are soldered to the PCB.

III. Version 1 Experimental Results

A. Recording From Dragonfly Nerve Cord

We performed initial tests of the version 1 telemetry system by recording neural activity from the target-selective descending neuron MDT1 [16] in the ventral nerve cord of a restrained dragonfly. A single 1.2-MΩ tungsten electrode was simultaneously monitored by using a conventional wired amplifier (AM Systems 3600, 40-kHz sampling) and a neural amplifier channel from the wireless telemetry unit (see Fig. 6). The data matched very closely. A background noise level of 11.5 $\mu\mathrm{V_{rms}}$ was observed by using the wired amplifier, while 12.1 $\mu\mathrm{V_{rms}}$ was observed by using the wireless telemetry unit (over a bandwidth of 300 Hz to 5 kHz).

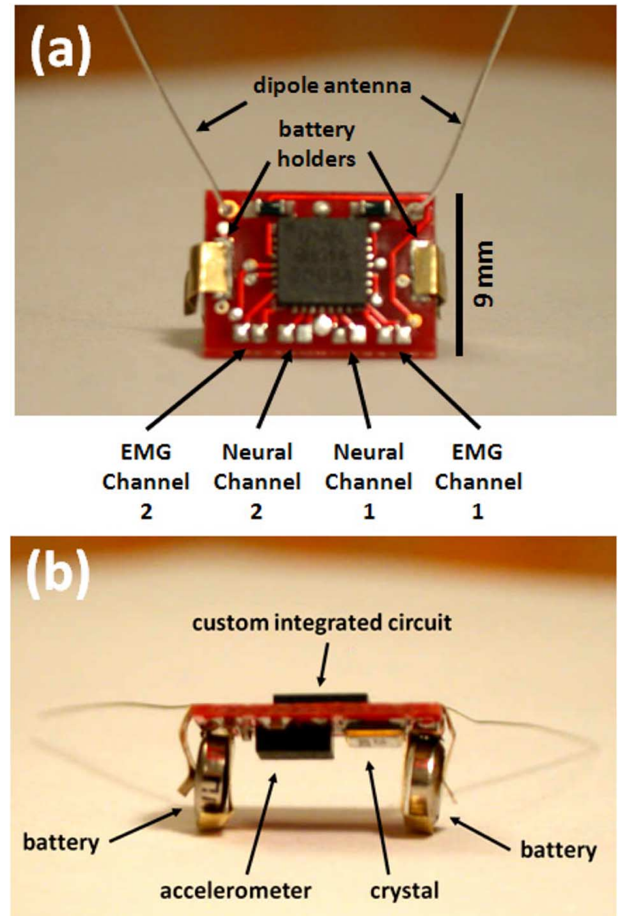

Fig. 5. (a) Complete 13×9 mm^2 version 1 telemetry system with a QFN-packaged chip. (b) Side view of the telemetry system showing an accelerometer and a crystal.

B. Recording From a Freely Jumping Locust

We used the version 1 wireless system to observe the activity evoked in an identified descending neuron (the DCMD) and two leg muscles in a locust presented with approaching objects simulated on a computer monitor [17]. The DCMD neuron is known to respond maximally to such stimuli, but its role in triggering escape behaviors remains unresolved, and its activity had never been recorded in freely escaping animals.

The telemetry system was affixed to the insect's cuticle using a mixture of rosin and beeswax. Teflon-coated Stablohm wires that measured 50 μm in diameter were used for extracellular recordings; insulation was removed at the ends (California Fine Wire, Grover Beach, CA). A hook-shaped electrode was implanted around the nerve cord and additional electrodes were inserted in the flexor and extensor muscles of the hindleg. See [17] for more details on the animal preparation.

Locusts were able to jump freely wearing the telemetry system (see Fig. 7), and data were not lost during the rapid

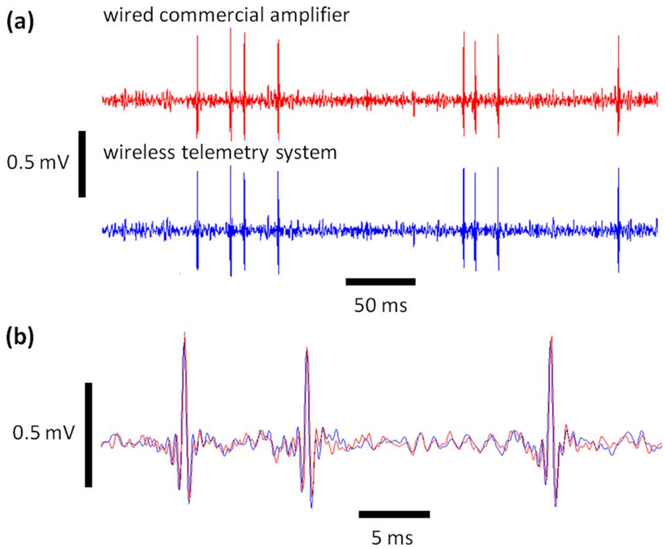

Fig. 6. (a) Extracellular recording of spiking activity from a neuron MDT1 in the dragonfly nerve cord by using a wired commercial amplifier (red) and wireless telemetry system (blue). (b) Close-up comparison of three spikes.

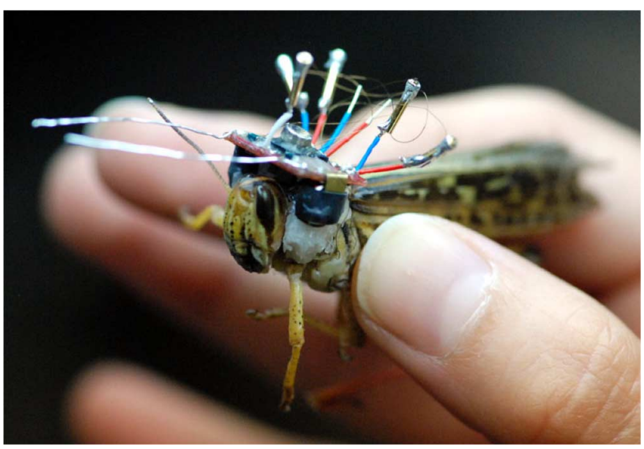

Fig. 7. Version 1 telemetry system mounted on a locust *Schistocerca americana*.

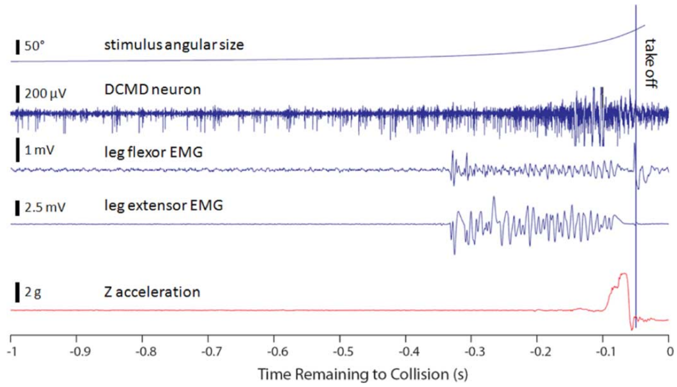

Fig. 8. Data obtained wirelessly from a freely jumping locust, in response to an expanding visual stimulus (top trace). A neural signal from the DCMD neuron, plus two EMG signals were monitored (middle traces). Accelerometer data show the jumping event (bottom trace).

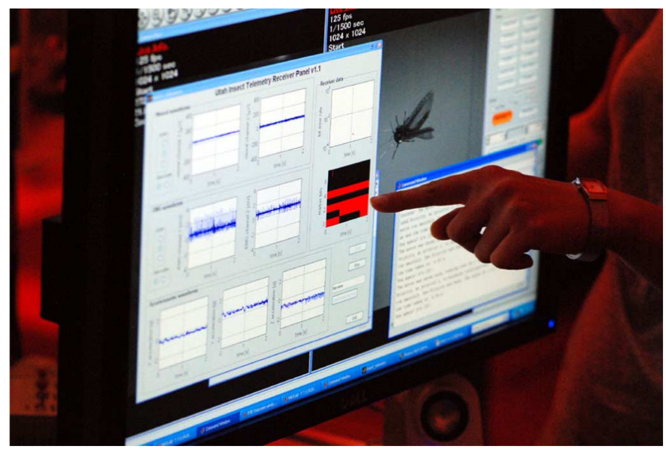

Fig. 9. Photograph of live wireless data acquisition from the locust flying in the wind tunnel. Wing beats are visible in EMG traces (center, to the left of the finger). High-speed video of the locust is synchronized to telemetry data.

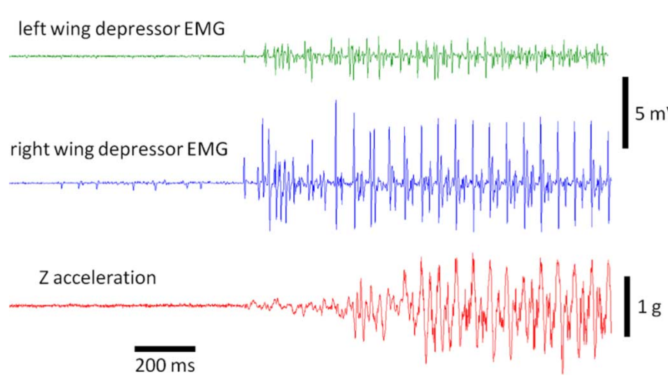

Fig. 10. Data obtained wirelessly from a loosely tethered locust flying in a wind tunnel. The onset of 18-Hz wing beats is observed in the two wing EMG traces (top) and acceleration trace (bottom).

movement. Fig. 8 shows sample recordings obtained from a freely jumping locust using this system. In this example, the locust jumps approximately 50 ms before the simulated time of collision. During the approach, the neuron's activity gradually increases and is followed by the co-activation of flexor and extensor muscles, and then jump acceleration. By varying the stimulus parameters and measuring the neural and muscle activities, we found that the muscle co-contraction is triggered once the DCMD activity and stimulus angular size reach a threshold level, and takeoff occurs after the extensor muscle generates enough spikes.

C. Recording From the Loosely Tethered Flying Locust

We have also used the system to observe wing muscle EMGs (and corresponding body acceleration) during loosely tethered flight in a low-speed wind tunnel (see Fig. 9). Muscle activity in the right and left wing depressor muscles occurs in synchrony with the wing beats (and corresponding body acceleration) at approximately 18 Hz during flight (see Fig. 10).

D. Recording From Freely Swimming Fish

The same system was made waterproof and used to obtain recordings from the skin of freely swimming weak electric fish

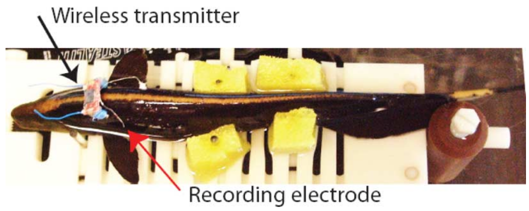

Fig. 11. Version 1 telemetry system mounted on a weak electric black ghost knife fish. To measure the transdermal potential, the recording electrode was implanted under the skin and the reference electrode was fixed across, over the fish's skin. (Electrodes are not implanted in this picture.)

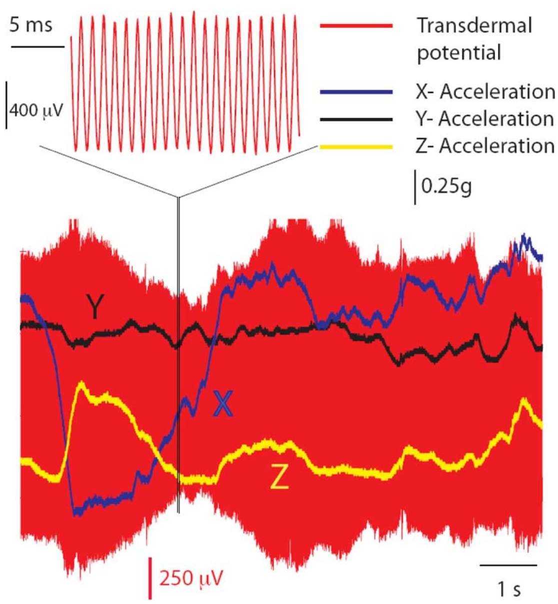

Fig. 12. Single channel of transdermal potential recording, and three-axis acceleration profiles obtained in a freely swimming black ghost knife fish. The amplitude of the carrier EOD waveform (magnified in top inset) is modulated due to the fish's swimming movements as well as changes in its distance relative to obstacles, such as tank walls.

Apteronotus albifrons, commonly known as black ghost knife fish (see Fig. 11). The circuit board was coated with liquid latex (Mehron, Inc., Chestnut Ridge, NY). Just before mounting the system on the fish, the batteries were secured by using heat-shrink tubing. Any remaining exposed area was covered using bee's wax and, finally, the entire board was sealed with high vacuum grease (Dow Corning Corp., Midland, MI).

Black ghost knife fish, which can measure up to 20–25 cm in length, possess an electric organ in their tails which generates a quasisinusoidal electric field around their body. Objects with a conductivity different from that of the water as well as the electric fields generated by other electric fish, create amplitude and phase modulations in the fish's electric organ discharge (EOD). These modulations are sensed by the electroreceptors that are distributed all over the fish's skin. Although the anatomy and physiology of the electrosensory system has been studied for many decades, and is very well characterized (see [18] for a review), the temporal dynamics of the input to electroreceptors in freely swimming fish are yet to be measured.

As a first step in studying natural electrolocation, it is therefore essential to monitor the input to the electrosensory system (i.e., the transdermal potential) in a freely swimming fish. Fig. 12 shows an example of such a recording using the wireless system described in this paper. The fish's own movements, apparent from the acceleration profile, generate amplitude modulations in the ~1-kHz carrier EOD wave (see inset), which was measured using the neural amplifiers. These recordings, combined with video tracking of the fish's body movement, can yield insights into the range and frequency of the EOD amplitude modulations during free swimming. As a next step, the EOD modulations can be studied in the context of prey capture and other natural behaviors. Using the same telemetry system, it will be possible to obtain recordings from the activity of the population of primary sensory neurons, as well as neurons in the next processing stages to study their firing properties in response to natural sensory input.

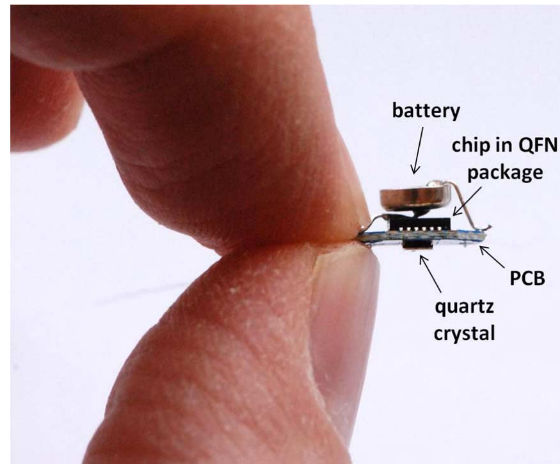

Fig. 13. Side view of the version 2 telemetry system with rigid 500-μm-thick PCB. The single 1.5-V battery accounts for 48% of the total system mass.

IV. Version 2 Telemetry System Design

A. IC Design

The use of a 3.0-V supply in the version 1 telemetry system required two batteries, which added to the size and mass of the unit. In an effort to build a smaller, lighter device, we redesigned the IC in a 0.35-μm CMOS technology with lower threshold voltages, which permitted operation at a single-battery 1.5-V supply. This process did not offer fast bipolar junction transistors, so we used nMOS transistors in place of the *npn* devices in the RF *LC* oscillator (see Q_1 and Q_2 in Fig. 3). Despite this handicap, the smaller parasitic capacitances in the 0.35-μm process allowed us to reduce overall current draw from 880 to 670 μA.

The version 2 chip also included a 9-b SAR ADC. The sampling rate and maximum range of the neural and EMG channels were identical to those shown for the version 1 chip (see Table I). The amplifier bandwidth and noise parameters were similar. An additional divide-by-2 stage was added after the crystal-oscillator circuit to permit operation with a 22.1184-MHz quartz crystal instead of the 11.0592-MHz crystals used in version 1. Higher frequency crystals are available in smaller sizes, and this change in the oscillator circuit allowed us to move from a 5.0×3.2 mm^2 crystal to a 2.5×2.0 mm^2 crystal.

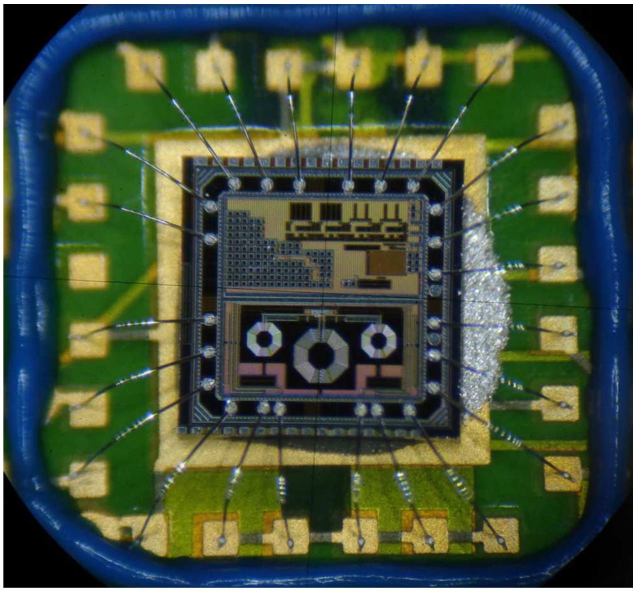

Fig. 14. Die photograph of a 1.88×1.88 mm^2 version 2 insect telemetry chip, fabricated in a 0.35-μm CMOS process and bonded directly to flex PCB. The three octagonal structures are on-chip inductors.

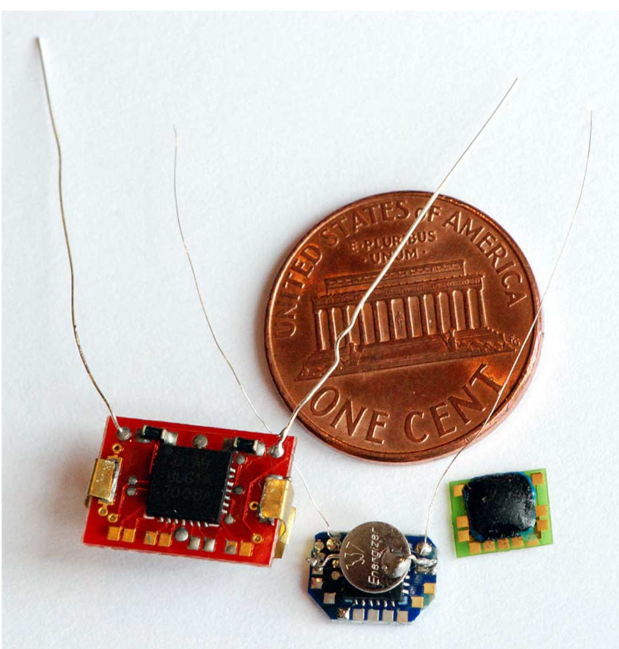

Fig. 15. Size comparison of 13×9 mm^2 version 1 system weighing 0.79 g (left); 9×6 mm^2 version 2 system with rigid PCB weighing 0.28 g (center); and 6×5 mm^2 version 2 system with flex PCB weighing 0.17 g (right). All weights include batteries. For clarity, the battery and antenna are not shown on the flex PCB system.

Reducing the supply voltage to 1.5 V precluded the use of an accelerometer, as no commercial accelerometers tolerating a supply voltage of less than 1.8 V could be found. However, eliminating the accelerometer allowed for further reductions in overall size and mass while extending battery life. In many scientific experiments, the data obtained by an accelerometer can be inferred by using video tracking. Also, flying insects often exceed the ±3-g range of the ADXL330 used in the version 1 system. For example, dragonflies regularly produce accelerations in the 1–6 g range during flight, and locusts routinely exceed 10 g during jumps.

TABLE II
MEASURED MASS BY COMPONENT

Component	Version 1 (rigid PCB)	Version 2 (rigid PCB)	Version 2 (flex PCB)
batteries	260 mg (2x E337)	130 mg (1x E337)	130 mg (1x E337)
battery holders	94 mg	10 mg	2 mg
printed circuit board	182 mg 13x9x0.50mm^3	70 mg 9x6x0.50mm^3	3 mg 6x5x0.03mm^3
chip (die only)	4 mg	3 mg	3 mg
chip packaging	62 mg 5x5 mm^2 QFN	37 mg 4x4 mm^2 QFN	n/a chip on board
quartz crystal	38 mg 5.0x3.2mm^2	9 mg 2.5x2.0mm^2	6 mg 2.0x1.6 mm^2
dipole antenna	32 mg (30 AWG)	7 mg (34 AWG)	7 mg (34 AWG)
accelerometer	56 mg	n/a	n/a
other components, solder, epoxy	62 mg	14 mg	21 mg
TOTAL	**790 mg**	**280 mg**	**172 mg**

B. *System-Level Design and Preliminary Experiments*

Moving to 0.35-μm fabrication technology reduced the die size to 1.88×1.88 mm^2 and allowed the chips to be packaged in a smaller 20-lead 4×4 mm^2 QFN package. The packaged chips were first mounted on a 9×6 mm^2 500-μm-thick rigid FR4 printed-circuit board (PCB) along with a single battery, crystal, and 34 AWG wire antenna (see Fig. 13). The complete version 2 system with battery and antenna weighs 0.28 g. The lower current draw of the version 2 chip, along with the lack of an accelerometer, extends battery life to 5 h.

In further efforts to reduce system mass, we fabricated a lightweight "flex" PCB using 25-μm-thick Kapton with 2-μm gold-plated copper traces. This reduced the PCB mass from 70 to 3 mg, and its dimensions to 6×5 mm^2. We also located a smaller 2.0×1.6 mm^2 22.1184-MHz crystal to use on the flex PCB. The board was designed to facilitate direct die-on-board assembly so that we could eliminate the weight associated with the QFN package (though some weight was added by the black epoxy used to cover and protect the bare die). Fig. 14 shows a photograph of a bare version 2 die bonded to a flex PCB. The complete version 2 system with flex board, battery, and antenna weighs 0.17 g; 76% of this mass is due to the single 1.5-V battery. Fig. 15 shows all three telemetry systems side by side for comparison. For clarity, the battery and antenna of the version 2 flex PCB system are not shown. Table II compares the mass breakdown of the complete version 1 system and the version 2 systems with rigid and flex PCBs.

The version 2 flex PCB unit has been attached to a medium-sized dragonfly (*Libellula lydia*) for preliminary neural recording experiments. Wireless data were collected from a target-selective descending neuron (TSDN) in the nerve cord by using a small tungsten electrode. Fig. 16 shows large

TABLE III
COMPARISON OF MINIATURE WIRELESS BIOPOTENTIAL RECORDING SYSTEMS

	Kutch [3]	**Fischer [4]**	**Kuwana [5]**	**Nieder [7]**	**Mohseni [6]**	**Takeuchi [8]**	**Mohseni [9]**	**Harrison version 1**	**Harrison version 2**
Supply voltage	1.5V	1.5 V	1.5V	2.8V	3.0V	3.0V	3.0V	3.0V	1.5V
Power consumption	–	–	–	–	2 mW	10 mW	2.2 mW	3.6 mW	1.0 mW
Approximate size	20x6mm^2	20x6mm^2	12x7mm^2	25x10mm^2	10x10mm^2	15x8mm^2	17x12mm^2	13x9mm^2	6x5mm^2
Total mass	0.42 g	0.55 g	0.4 g	3.1 g w/out batt.	0.74 g	0.1 g w/out batt.	1.1 g	0.79 g	0.17 g
Battery life	–	–	0.5 h	–	3 h	0.5 h	–	2 h	5 h
Signals transmitted	1 EMG	2 EMG	2 EMG	2 neural	2 EMG	1 neural	3 neural	2 neural 2 EMG 3 accel.	2 neural 2 EMG
Telemetry frequency	145 MHz	145 MHz	80 MHz	100 MHz	100 MHz	85 MHz	96 MHz	920 MHz	905 MHz
Telemetry modulation	analog FM	analog FM	analog FM	analog FM	analog FM	analog FM	analog FM	digital FSK	digital FSK
Telemetry range	~25 m	>20 m	–	"few meters"	~2 m	~16 m	0.5 m	~2 m	~2 m
Number/type of integrated circuits	0	0	0	3 standard off-the-shelf	0	1 standard off-the-shelf	1 custom 1.5µm CMOS	1 custom 0.6µm BiCMOS; 1 MEMS accel.	1 custom 0.35µm CMOS
Number of discrete (off-chip) components	12	24	14	25	32	18	3	7	1
Target animal(s)	locust	locust	moth	owl	moth	cockroach	marmoset	locust; elec. fish; dragonfly	locust; elec. fish; dragonfly
Year of publication	1993	1996	1999	2000	2001	2004	2005	2010	2011

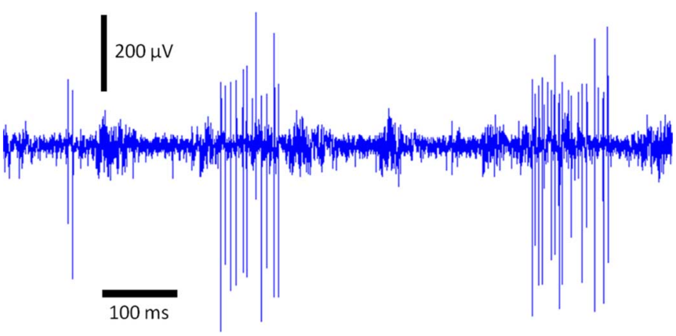

Fig. 16. Neural action potentials recorded wirelessly from a target-selective descending neuron using the version 2 telemetry system on an untethered, perched dragonfly.

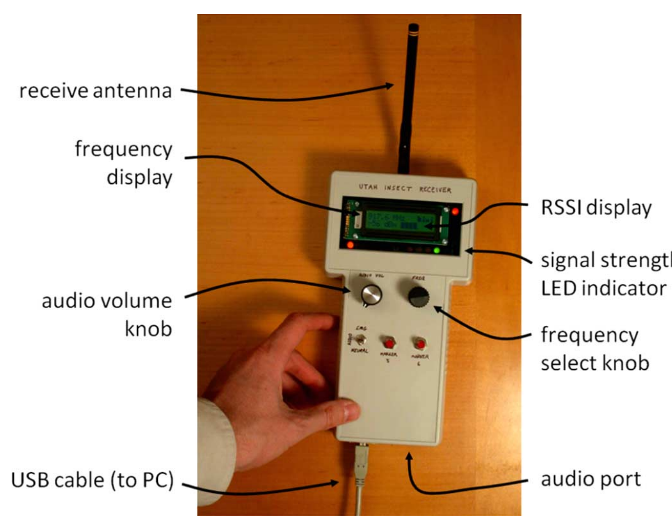

Fig. 17. Custom wireless telemetry receiver with a USB interface to a PC.

neural action potentials observed in the TSDN neuron of an untethered, perched dragonfly.

V. CONCLUSION

We have presented two miniature wireless telemetry systems that demonstrate one step in the development of new scientific instrumentation. Reducing the supply voltage to 1.5 V by moving to a smaller process node allowed for significant size and mass reduction at the expense of the accelerometer. Low-voltage MEMS accelerometers and gyroscopes would be of great use in building miniature telemetry systems. An operation down to 1.4 V is desirable since 1.5-V batteries rarely provide precisely 1.5 V (see Fig. 1). The range of these inertial sensors should be scaled to match the dynamics of the animals under study.

Fig. 17 shows the custom RF receiver with a universal-serial-bus (USB) interface built to collect the wireless data. An audio port allows for real-time monitoring of neural or EMG signals over headphones during experiments. Since an open-loop *LC* oscillator was used to set the RF transmitter frequency, the receiver frequency occasionally must be changed to follow drifts in the transmit frequency caused by changes in temperature, supply voltage, or antenna impedance. Adding an on-chip PLL could lock the transmit frequency to a multiple of the crystal frequency and eliminate the need for receiver tuning, at the expense of greater power consumption and, thus, reduced battery life.

Table III compares the size, mass, and performance of nine miniature telemetry systems reported in the literature, including the systems presented here. All systems presented in this table have masses of less than 4 g and consume 10 mW or less, permitting operation with small and/or flying animals. Larger telemetry systems transmitting between 16 and 64 neural signals and having masses in the 30–60 g range have recently been reported for use with rats [19]–[21]. These high-channel-count systems consume more than 100 mW of power, and so require substantially larger battery packs to provide a few hours of operation.

The small size and low mass of wireless telemetry devices based around custom ICs are enabling new experiments in the study of the neural control of behavior. An important requisite for the development of these systems is the close interaction between the electrical engineers who design the circuitry and the biologists who become the end users of the device. Only by working together can the proper tradeoffs between size, mass, battery life, and performance be made in a satisfactory manner.

ACKNOWLEDGMENT

The second author would like to thank Dr. R. Krahe for his support with the electric fish segment of this project.

REFERENCES

[1] G. K. Taylor and H. G. Krapp, "Sensory systems and flight stability: What do insects measure and why?," *Adv. Insect Physiol.*, vol. 34, pp. 231–316, 2008.

[2] R. Olberg, R. C. Seaman, M. I. Coats, and A. F. Henry, "Eye movements and target fixation during dragonfly prey interception flights," *J. Comp. Physiol. A*, vol. 193, no. 7, pp. 685–693, 2007.

[3] W. Kutsch, G. Schwarz, H. Fischer, and H. Kautz, "Wireless transmission of muscle potentials during free flight of a locust," *J. Exp. Biol.*, vol. 185, pp. 367–373, 1993.

[4] H. Fischer, H. Kautz, and W. Kutsch, "A radiotelemetric 2-channel unit for transmission of muscle potentials during free flight of the desert locust, *Schistocerca gregaria*," *J. Neurosci. Meth.*, vol. 64, pp. 39–45, 1996.

[5] Y. Kuwana, N. Ando, R. Kanzaki, and I. Shimoyama, "A radiotelemetry system for muscle potential recordings from freely flying insects," in *Proc. BMES/EMBS Conf.*, Oct. 1999, vol. 2, p. 846.

[6] P. Mohseni, K. Nagarajan, B. Ziaie, K. Najafi, and S. B. Crary, "An ultralight biotelemetry backpack for recording EMG signals in moths," *IEEE Trans. Biomedical Eng.*, vol. 48, no. 6, pp. 734–737, Jun. 2001.

[7] A. Nieder, "Miniature stereo radio transmitter for simultaneous recording of multiple single-neuron signals from behaving owls," *J. Neurosci. Meth.*, vol. 101, pp. 157–164, 2000.

[8] S. Takeuchi and I. Shimoyama, "A radio-telemetry system with a shape memory alloy microelectrode for neural recording of freely moving insects," *IEEE Trans. Biomed. Eng.*, vol. 51, no. 1, pp. 133–137, Jan. 2004.

[9] P. Mohseni, K. Najafi, S. J. Eliades, and X. Wang, "Wireless multichannel biopotential recording using an integrated FM telemetry circuit," *IEEE Trans. Neural Syst. Rehab. Eng.*, vol. 13, no. 3, pp. 263–271, Sep. 2005.

[10] M. Wikelski, D. Moskowitz, J. S. Adelman, J. Cochran, D. S. Wilcove, and M. L. May, "Simple rules guide dragonfly migration," *Biol. Lett.*, vol. 2, pp. 325–329, 2006.

[11] J. Mavoori, B. Millard, J. Longnion, T. Daniel, and C. Diorio, "A miniature implantable computer for functional electrical stimulation and recording of neuromuscular activity," in *Proc. IEEE Int. Workshop Biomed. Circuits Syst.*, Dec. 2004, pp. 13–16.

[12] D. C. Daly, P. P. Mercier, M. Bhardwaj, A. L. Stone, J. Voldman, R. B. Levine, J. G. Hidebrand, and A. P. Chandrakasan, "A pulsed UWB receiver SoC for insect motion control," in *Proc. ISSCC Dig. Tech. Papers*, Feb. 2009, pp. 200–201.

[13] R. R. Harrison, H. Fotowat, R. Chan, R. J. Kier, A. Leonardo, and F. Gabbiani, "A wireless neural/EMG telemetry system for freely moving insects," in *Proc. IEEE Intl. Symp. Circuits Syst.*, Paris, France, 2010, pp. 2952–2955.

[14] R. R. Harrison and C. Charles, "A low-power, low-noise CMOS amplifier for neural recording applications," *IEEE J. Solid-State Circuits*, vol. 38, no. 6, pp. 958–965, Jun. 2003.

[15] R. R. Harrison, "The design of integrated circuits to observe brain activity," *Proc. IEEE*, vol. 96, no. 7, pp. 1203–1216, Jul. 2008.

[16] R. M. Olberg, "Identified target-selective visual interneurons descending from the dragonfly brain," *J. Comp. Physiol. A*, vol. 159, no. 6, pp. 827–840, 1986.

[17] H. Fotowat, R. R. Harrison, and F. Gabbiani, "Muliplexing of motor information in the discharge of a collision detecting neuron during escape behaviors," *Neuron*, vol. 69, pp. 147–158, 2011.

[18] , T. H. Bullock, C. D. Hopkins, A. N. Popper, and R. R. Fay, Eds., *Electroreception*. New York: Springer, 2005.

[19] R. E. Hampson, V. Collins, and S. A. Deadwyler, "A wireless recording system that utilizes Bluetooth technology to transmit neural activity in freely moving animals," *J. Neurosci. Meth.*, vol. 182, pp. 195–204, 2009.

[20] E. Greenwald, M. Mollazadeh, N. Thakor, W. Tang, and E. Culurciello, "A VLSI neural monitoring system with ultra-wideband telemetry for awake behaving subjects," in *Proc. IEEE Int. Symp. Circuits Syst.*, Paris, France, 2010, pp. 1193–1196.

[21] T. A. Szuts, V. Fadeyev, S. Kachiguine, A. Sher, M. V. Grivich, M. Agrochão, P. Hottowy, W. Dabrowski, E. V. Lubenov, A. G. Siapas, N. Uchida, A. M. Litke, and M. Meister, "A wireless multi-channel neural amplifier for freely moving animals," *Nature Neurosci.*, vol. 14, no. 2, pp. 263–270, Feb. 2011.

Reid R. Harrison (S'98–M'00) received the B.S. degree in electrical engineering from the University of Florida, Gainesville, in 1994 and the Ph.D. degree from the California Institute of Technology, Pasadena, in 2000.

He joined the University of Utah, Salt Lake City, in 2000, where was an Associate Professor of Electrical and Computer Engineering and an Adjunct Associate Professor of Bioengineering through 2010. In 2003, he founded Intan Technologies, LLC and joined them full time in 2010. His research interests include low-power analog and mixed-signal complementary metal–oxide semiconductor circuit design, integrated electronics for neural interfaces, and other biomedical devices and hardware for biologically inspired computational systems.

Dr. Harrison received the Jack Raper Award for Outstanding Technology Directions Paper from the International Solid-State Circuits Conference (ISSCC) in 2006. He has served on the technical program committees of ISSCC and the IEEE International Symposium on Circuits and Systems (ISCAS).

Haleh Fotowat (S'00–M'08) received the B.S. degree in electrical engineering from Tehran Polytechnic, Tehran, Iran, in 2000, the M.S. degree in electrical engineering from the University of Houston, Houston, TX, in 2002, and the Ph.D. degree in neuroscience in 2010 from Baylor College of Medicine, Houston.

Currently, she is a Postdoctoral Fellow at McGill University, Montreal, QC, Canada. Her research interests include the sensory-motor transformations underlying natural behavior, the role of neuromodulators in shaping sensory responses, and the use of wireless telemetry systems for studying these responses in freely behaving animals.

Dr. Fotowat received the Grass Foundation Fellowship in Neuroscience in 2010.

Raymond Chan received the B.Sc. degree in computational science (Hons.) from the Australian National University, Canberra, Australia, in 2005 and the Ph.D. degree in biomathematics from the Max Planck Institute for Mathematics in the Natural Sciences and the University of Leipzig, Leipzig, Germany, in 2008.

Currently, he is a Postdoctoral Associate at Baylor College of Medicine, Houston, TX, working on the aerodynamics and neuroscience of insect flight.

Ryan J. Kier (S'03–M'09) received the B.S. and M.S. degrees in electrical engineering from the University of Utah, Salt Lake City, in 2004 and the Ph.D. degree in electrical engineering from the University of Utah in 2010.

While working toward the Ph.D. degree, he completed two integrated-circuit (IC) design internships with SliceX (now SiFlare) in 2006 and Medtronic in 2007. Since 2008, he has been a Senior Member of Technical Staff with SiFlare (formerly SliceX), Salt Lake City. His design interests are in high-speed, high-resolution pipelined analog-to-digital converters, switched capacitor circuits, and low-jitter clocking.

Dr. Kier was a co-recipient of the Jack Raper Award for Outstanding Technology-Directions Paper at ISSCC 2006 in 2007.

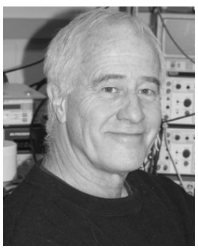

Robert Olberg received the B.S. degree in biology at Rice University, Houston, TX, in 1968 and the Ph.D. degree in zoology from the University of Washington, Pullman, in 1978.

After a postdoctoral appointment at the Max-Planck-Institut für Verhaltensphysiologie, Seewiesen, Germany, he joined the faculty at Union College, Schenectady, NY, where he is currently the Florence B. Sherwood Professor of Life Sciences. He has worked with his undergraduate research students on the sensory systems of a variety of insects, but most notably the visual control of flight in dragonflies, with studies in his lab ranging from the analysis of single neuron activity to flight behavior. His work has been funded by the National Science Foundation, Research Corporation, U.S. Department of Agriculture, Air Force Office of Scientific Research, and Howard Hughes Medical Institute. Currently, he has a Visiting Scientist appointment at the Janelia Farm Research Campus of the Howard Hughes Medical Institute, working with Dr. Anthony Leonardo.

Anthony Leonardo received the B.S. degree in cognitive science from Carnegie Mellon University, Pittsburgh, PA, and the Ph.D. degree in computation and neural systems from the California Institute of Technology, Pasadena, in 2002.

He then completed postdoctoral work at Bell Labs and Harvard University. Since 2008, he has been a Group Leader at the Janelia Farm Research Campus of the Howard Hughes Medical Institute, where his lab explores the principles underlying neural information processing. His current research focuses on the computations neural circuits implementation, how robust they are, and how different circuits are linked into systems to produce complex behaviors. These questions are pursued in the context of prey capture in salamanders and dragonflies.

Dr. Leonardo received the Lindsley Prize in Behavioral Neuroscience, the Capranica Prize in Neuroethology, a Helen Hay Whitney Fellowship, and the Burroughs-Wellcome Career Award in the Biological Sciences.

Fabrizio Gabbiani received a Diploma and Ph.D. degree in mathematical physics from the Swiss Federal Institute of Technology (ETH), Zürich, Switzerland.

He was a Postdoctoral Fellow at the California Institute of Technology, Pasadena, before joining the faculty of Baylor College of Medicine, Houston, TX. Currently, he is an Associate Professor in the Department of Neuroscience and holds an adjunct appointment in the Department of Computational and Applied Mathematics at Rice University, Houston. His research focuses on insect vision and behavior as well as computational neuroscience.